



HAL
open science

Rare Earth Elements binding to humic acids: NICA-Donnan model parameterization

Alba Otero-Fariña, Noémie Janot, Remi Marsac, Charlotte Catrouillet, Jan E
Groenenberg

► To cite this version:

Alba Otero-Fariña, Noémie Janot, Remi Marsac, Charlotte Catrouillet, Jan E Groenenberg. Rare Earth Elements binding to humic acids: NICA-Donnan model parameterization. *Environmental Chemistry*, In press, 21 (1), pp.EN23049. 10.1071/EN23049 . hal-04184021

HAL Id: hal-04184021

<https://hal.science/hal-04184021>

Submitted on 21 Aug 2023

HAL is a multi-disciplinary open access archive for the deposit and dissemination of scientific research documents, whether they are published or not. The documents may come from teaching and research institutions in France or abroad, or from public or private research centers.

L'archive ouverte pluridisciplinaire **HAL**, est destinée au dépôt et à la diffusion de documents scientifiques de niveau recherche, publiés ou non, émanant des établissements d'enseignement et de recherche français ou étrangers, des laboratoires publics ou privés.

Rare Earth Elements binding to humic acids:

NICA-Donnan model parameterization

Alba Otero-Fariña^{1,a}, Noémie Janot^{1,2,3}, Rémi Marsac⁴, Charlotte
5 Catrouillet⁵, Jan E. Groenenberg^{1,6,*}

¹ CNRS, Université de Lorraine, LIEC – UMR 7360, Vandœuvre-lès-Nancy, F-54501, France.

² INRAE, Université de Lorraine, LSE – UMR 1120, Vandœuvre-lès-Nancy, F-54501, France.

10 ³ INRAE, Bordeaux Sciences Agro, ISPA – UMR 1391, Villenave d'Ornon F-33140, France.

⁴ Univ. Rennes, CNRS, Géosciences Rennes – UMR 6118, Rennes F-35000, France

⁵ Université Paris Cité, CNRS, Institut de Physique du Globe de Paris, Paris F-75005, France

⁶ Soil Chemistry and Chemical Soil Quality group, Department of Environmental Sciences,
Wageningen University, PO Box 47, 6700 AA Wageningen, The Netherlands.

15

Present address:

^a School of Earth and Environment, University of Leeds, Leeds LS2 9JT, UK.

20

* Correspondence to:

bertjan.groenenberg@wur.nl

25 Environmental Context

Rare earth elements (REEs) are technologically-critical elements released into the environment by various anthropogenic activities, and whose ecotoxicological impacts are still relatively unknown. REE binding to natural organic matter (NOM) is key to understand their fate and bioavailability in the environment. With this work, it is now possible to predict REE binding to NOM in various
30 environments using various speciation software (ECOSAT, ORCHESTRA, Visual MINTEQ).

Abstract

Rationale:

35 Understanding REE speciation in different natural environments is important to evaluate their environmental risks since different chemical species of an element may have different bioavailability and toxicity. REEs have a great affinity for particulate- and dissolved organic matter, particularly fulvic and humic acids (HA). Thus, the use of humic ion-binding models may help to understand and predict the behaviour and speciation of these species in surface waters,
40 groundwaters, and soils.

Methodology:

In this work, we used previously published experimental datasets to parametrize the NICA-Donnan (ND) model for REEs binding with HA, using the model optimization tool PEST-ORCHESTRA. We propose to use linear-free energy relationships (LFER) to constrain the number of parameters
45 to optimize.

Results:

We determined a coherent ND parameter set for the whole REEs series being compatible with available generic ND parameters for other metals. The impact of pH, ionic strength, REE/HA ratio as well as the presence of competitors (Fe^{3+} , Al^{3+} and Cu^{2+}) on model results is analysed.

50 *Discussion:*

We consolidate the confidence in our derived ND parameters for REE by comparing with the Irving-Rossotti LFER. We also showed the general applicability of this relationship to predict and constrain metal-binding parameters for the NICA-Donnan model. We discuss observed shortcomings and come with suggestions for potential improvement of NICA-Donnan modelling.

55

Keywords

speciation, trace metals, soil chemistry, water chemistry

Introduction

Rare earth elements (REEs) have been increasingly used in the past decades. They are
60 technologically critical elements used in high-tech products such as lasers, storage media for data
handling, mobile phones, photovoltaic cells, catalyser in cars, permanent magnets in turbines,
lodestones, or ceramics manufacturing. Anthropogenic activities such as mining, industrial
manufacturing, but also agriculture can increase the release of these emerging pollutants into the
environment (Borgmann *et al.*, 2005; Vukov, Smith and McGeer, 2016; Liu *et al.*, 2017). Despite
65 evidenced ecotoxicological effects of REEs on various organisms (Gonzalez *et al.*, 2014; González
et al., 2015; Oral *et al.*, 2017; Gwenzi *et al.*, 2018; Romero-Freire *et al.*, 2018, 2021; Pagano *et al.*,
2019; Malhotra *et al.*, 2020), the fate and behaviour of the REEs - and thus their impact on
different ecosystems - are still relatively unknown (Kouhail, Dror and Berkowitz, 2019; Batley *et al.*,
2022). Understanding their speciation in different natural environments is very important to
70 evaluate their ecotoxicological risks since their different chemical species have different
bioavailabilities and toxicities (Leybourne and Johannesson, 2008; Migaszewski and Galuszka,
2015; Khan *et al.*, 2016; Romero-Freire *et al.*, 2019; Malhotra *et al.*, 2020; Lachaux *et al.*, 2022).
REEs in natural waters or soils are often operationally distributed between (i) truly dissolved, (ii)
colloidal, and (iii) particulate fractions (Singhal *et al.*, 2006). On both colloids and particulate
75 fractions, REE partitioning has been attributed to adsorption to organic- and mineral phases or
precipitation. REE concentrations in the different phases depend on pH, ionic strength, redox
conditions, and types of minerals present in the environment, which impact the complexation of
REEs with organic and inorganic ligands (Johannesson *et al.*, 2004; Leybourne and Johannesson,
2008; Pourret *et al.*, 2010; Liu *et al.*, 2017). Thus, solid-solution partitioning, mineral equilibria
80 and solution speciation of REEs are critical factors to determine their solubility in soils, sediments

and waters and thereby their environmental fate and diffusion, mobility, bioavailability and toxicity (Groenenberg and Lofts, 2014).

REEs form a homogeneous group of elements, with coherent behaviour among the series, generally divided in 3 groups: light REE (LREE, from La to Nd), Middle REE (MREE, from Nd
85 to Tb) and heavy REE (HREE, from Dy to Lu). They have a great affinity for particulate- and dissolved organic matter, particularly humic- and fulvic acids therein (Sonke and Salters, 2006; Pourret *et al.*, 2007; Marsac *et al.*, 2011; Gangloff *et al.*, 2014; Catrouillet *et al.*, 2019). Humic ion-binding models are powerful tools developed to understand and predict the behaviour and speciation of trace metals including REEs and radionuclides in surface waters, groundwaters, and
90 soils, and interactions of potentially toxic trace elements with biota (Groenenberg and Lofts, 2014; Di Bonito, Lofts and Groenenberg, 2018). These models consider both the heterogeneous nature of the humic substances (HSs) and electrostatic interactions due to their negative charge. Humic Acids (HA) contain functional groups, mainly carboxylic and phenolic groups, that have a high affinity to bind trace metals. Binding site heterogeneity can be described, depending on the model,
95 with a discrete- (Model VI and VII (Tipping, 1998; Lofts and Tipping, 2011), Stockholm Humic Model (Gustafsson, 2001) or with a continuous distribution, as in the Non-Ideal Competitive Adsorption (NICA)-Donnan model (Kinniburgh *et al.*, 1999; Koopal *et al.*, 2005). Binding parameters for all REEs have been determined for Model VII (Tipping, Lofts and Sonke, 2011) and recently refined by Marsac *et al.* (2021) by using previously published datasets (Sonke and
100 Salters, 2006; Pourret *et al.*, 2007; Marsac *et al.*, 2010). For NICA-Donnan (ND), to this day only Eu and Dy parameters are available (Milne *et al.*, 2003). Here, we use the same datasets as used by Marsac *et al.* (2021) to derive ND model parameters for REEs binding with HA, using the model optimization tool PEST-ORCHESTRA (Janot *et al.*, 2017).

The number of parameters to be optimized in the ND model fit is, however, generally too large to
105 find an unconditional fit using titration and adsorption data. Parameter constraints could help
reduce parameter uncertainty and obtain a coherent set of model parameters across different
elements (Tipping, 1998, 2002; Kinniburgh *et al.*, 1999; van Riemsdijk *et al.*, 2006; Lenoir,
Matynia and Manceau, 2010). Here we look for possibilities to constrain the fits using linear free
energy relations (or Gibbs energy relations, LFER) that, empirically, relate model parameters to
110 thermodynamic constants. In this work we include, (i) the use of LFER developed by Milne *et al.*
(2003) who related ND parameters for metal cation to their first hydrolysis constants, and (ii) the
evaluation of the applicability of the approach developed by Tipping *et al.* (2011) for binding
constants in Humic Ion Binding Model VII to be applied for ND. The latter approach, based on
the study of Carbonaro and Di Toro (2007) makes use of the Irving–Rossotti approach (Irving *et*
115 *al.*, 1956) and was recently extended for REEs by Marsac *et al.* (2021). Once the model parameters
for different elements are obtained, it is also interesting to model data for competition experiments
of the REEs with other metals (such as Fe^{3+} , Al^{3+} and Cu^{2+}) to test the coherency of the obtained
model parameters for different elements. This work aims to provide parameters to estimate REE
binding to HA in various physico-chemical conditions of pH, concentrations and ionic strengths
120 (I), in the framework of an advanced humic-ion binding model, NICA-Donnan. It will aid for the
calculation of REE speciation in various environments and therefore better understanding the
environmental behaviour of these critical elements.

Materials and methods

125 NICA-Donnan model

The NICA-Donnan model is explained elsewhere in detail (Kinniburgh *et al.*, 1999; Koopal *et al.*, 2005). The NICA equation describes the local adsorption isotherm for specific binding of cations to the reactive sites of humic substances, while the Donnan model accounts for the electrostatic interactions. Briefly, the expression of the consistent NICA model for multi-component
130 competitive binding states that Q_i , the amount of a component i bound to the HS, at solution concentration c_i , is given by the equation (1):

$$Q_i = \frac{n_{i,1}}{n_{H,1}} \times Q_{max,1} \frac{(\tilde{K}_{i,1} c_i)^{n_{i,1}}}{\sum_i (\tilde{K}_{i,1} c_i)^{n_{i,1}}} \times \frac{[\sum_i (\tilde{K}_{i,1} c_i)^{n_{i,1}}]^{p_1}}{1 + [\sum_i (\tilde{K}_{i,1} c_i)^{n_{i,1}}]^{p_1}} \\ + \frac{n_{i,2}}{n_{H,2}} \times Q_{max,2} \frac{(\tilde{K}_{i,2} c_i)^{n_{i,2}}}{\sum_i (\tilde{K}_{i,2} c_i)^{n_{i,2}}} \times \frac{[\sum_i (\tilde{K}_{i,2} c_i)^{n_{i,2}}]^{p_2}}{1 + [\sum_i (\tilde{K}_{i,2} c_i)^{n_{i,2}}]^{p_2}}$$

(1)

135 In this framework, two types of functional groups are considered, type 1 sites with a relative low affinity for cation binding (carboxylic type groups) and type 2 sites with a relative high-affinity for cation binding (phenolic type sites). $Q_{max,i}$ corresponds to the maximum adsorption capacity of each type of site, n_i reflects the non-ideality of the system, related to lateral interactions and/or stoichiometric effects and is specific to each ion i ($0 < n_i \leq 1$, where 1 is the ideal case), p is the
140 width of the affinity distribution for each type of sites, and \tilde{K}_i is the median of the distribution of each type of sites and the ion i .

Thus, from the NICA equation, four parameters are needed to describe the site density and site heterogeneity of the humic material with: $Q_{max,1}$ and $Q_{max,2}$ being the site densities (in mol kg⁻¹), and p_1 and p_2 representing the heterogeneity of the type 1- and type 2-sites of the humic material,

145 respectively. The other four parameters are needed to describe ion-specific binding (proton or metal): $\tilde{K}_{i,1}$, $\tilde{K}_{i,2}$, $n_{i,1}$, and $n_{i,2}$, which describe the median affinities and non-idealities of the ion-binding, respectively.

This NICA equation can be combined with electrostatic interactions by using the local concentration of species i at the binding sites $c_{i,loc}$ instead of the bulk concentration c_i . This has
 150 generally been done using the Donnan model, which considers that HSs behave as a homogeneously charged gel with a constant potential Ψ_D (V) in which the concentration of an ion $c_{i,D}$ (mol L⁻¹) is related to its bulk solution concentration c_i (mol L⁻¹) according to the following equation:

$$c_{i,D} = c_i \cdot \exp\left(\frac{-z_i F \Psi_D}{RT}\right) \quad (2)$$

155 Where F , R and T are the Faraday constant, gas constant and absolute temperature, respectively. In this electrostatic model, we consider that the charge of the HS particle Q is counteracted by the accumulation of counter-ions and the exclusion of co-ions within this Donnan gel of volume V_D (L kg⁻¹). The corresponding charge neutrality can be written as:

$$\frac{Q}{V_D} + \sum_i z_i (c_{i,D} - c_i) = 0 \quad (3)$$

160 The Donnan volume is needed to be able to solve these equations. It has been shown to evolve with I according to the following empirical equation (Benedetti, Van Riemsdijk and Koopal, 1996):

$$\log V_D = \alpha + \beta \log I \quad (4)$$

where α and β are empirical constants. Later, a simpler relation has been introduced, with only
 165 one empirical adjustable parameter that varies amongst HSs (Kinniburgh *et al.*, 1999):

$$\log V_D = b(1 - \log I) - 1 \quad (5)$$

where b is an empirical adjustable parameter that varies amongst HSs (Kinniburgh *et al.*, 1999) Milne *et al.* (2001, 2003) compiled a large dataset of available acid/base titration- and metal sorption data for HA and FA to derive their ND parameters for FA and HA proton and metal binding. First the ND model was fitted to the individual HA titration data to obtain HA specific ND proton parameters using equation (5) for the relation between V_D and I . The averaged ND proton parameters were then used to fit the available data (various HA) for each separate metal simultaneously. The thus obtained “generic” ND parameters are now used in various speciation codes including ECOSAT, Visual MINTEQ and ORCHESTRA. Therefore, we followed the approach of Milne *et al.* to have our newly derived REE parameters compatible with their generic parameter set.

Datasets used for parameterization

Four datasets were used to calibrate the NICA-Donnan model parameters for REEs binding to HA, for a total of 55 different measurements (Sonke and Salters, 2006; Pourret *et al.*, 2007; Marsac *et al.*, 2010, 2012). These datasets are, to our knowledge, the only ones that cover the whole REEs series, and over a wide range of pHs and metal loadings. They were already used by Marsac *et al.* to calibrate the Models VI and VII HA-REEs parameters (Marsac *et al.*, 2011, 2021). The experimental conditions in which these datasets were obtained are summarized below and in **Table 1**.

Sonke and Salters dataset

Sonke and Salters (2006) conducted REEs-HA binding experiments for each of the 14 naturally present REEs separately. They used a standard Leonardite HA (a coal humic acid from the International Humic Substances Society, code 1S104H). REE binding to HA was studied with
190 EDTA competition coupled with capillary electrophoresis-ICP-MS analysis. This study provides a dataset at low metal loadings and slightly acidic to basic pH values (6-9) at 0.1 M NaNO₃, and an extra series at pH 7 and 0.01 M NaNO₃ (**Table 1**).

Pourret *et al.* dataset

Differently from the previous dataset, Pourret *et al.* (2007) conducted REEs-HA binding
195 experiments for all the REEs together. The experiments were performed at pH 2 – 10.5, fixed ionic strength (0.001 M NaNO₃) and concentration of REEs (50 µg L⁻¹), and 3 different concentrations of HA. The synthetic Aldrich HA was purified (PAHA) according to the protocol of Vermeer *et al.* (1998), using acid (HF and HCl) and resin (Dowex 50W-X8) washing steps to remove soluble minerals and trace metals, respectively. Truly dissolved REE was separated from REE bound to
200 HA by ultrafiltration and measured with ICP-MS (**Table 1**).

Marsac *et al.* 2010 dataset

Marsac *et al.* (2010) used the Pourret *et al.* (2007) ultrafiltration method to study the metal loading effect on REEs binding to the same PAHA. The PAHA solution was additionally purified by ultrafiltration at 10kDa in order to remove potential small molecules that could pass through the
205 ultrafiltration membrane in the REE-PAHA binding experiments (Marsac *et al.*, 2010). They also performed their experiments with all the REEs together, under acidic conditions (pH = 3) and

constant ionic strength (I) of 0.01 M NaCl (**Table 1**), being ten times higher than that used by Pourret et al. (2007).

Marsac et al. 2012 dataset

210 Using the same experimental method as Marsac et al. (2010), Marsac *et al.* (2012) performed experiments at constant concentrations of REEs ($\sum[\text{REE}] = 10 \mu\text{M}$), HA ($[\text{PAHA}] = 12.2 \text{ mg L}^{-1}$) and ionic strength (I = 0.01 M NaCl) but varying pH between 3 and 6.

In subsequent studies, Marsac *et al.* developed this dataset to investigate independently the effect of Fe, Al, and Cu on REE binding to PAHA (Marsac *et al.*, 2012, 2013, 2021), using the same

215 metal concentrations $[\text{Al/Fe/Cu}] = 10 \mu\text{M}$.

Table 1. Summary of the datasets used in this study to derive NICA parameters for REE

Dataset	Sonke & Salters	Pourret <i>et al.</i>	Marsac <i>et al.</i> 2010	Marsac <i>et al.</i> 2012
Number of data points per REE	5	28	15	7
pH range	6 - 9	2.2 - 10.4	3	3-6
HA used	Leonardite HA	Purified Aldrich HA	Purified Aldrich HA	
HA concentration (mg L ⁻¹)	10	5 ; 10 ; 20	5 - 45	12.2
REE concentration (µg L ⁻¹)	12.5	50	2 - 120	110
REE/HA ratio (mg g ⁻¹)	2.5	2.5 ; 5 ; 10	0.2 - 12.6	9
I (M)	0.01; 0.1	0.001	0.01	0.01
Experimental approach	EDTA competition coupled with capillary electrophoresis-ICP-MS analysis on single REE-HA system	Ultrafiltration on multi REE-HA system		

Parameterization approach

220 ND fitting procedure

We used the generic ND proton parameters derived by Milne *et al.* (Milne, Kinniburgh and Tipping, 2001; Milne *et al.*, 2003) (values reminded in Table S1) and fitted only the metal-ion binding parameters. We used the PEST-ORCHESTRA tool (Janot *et al.*, 2017) to fit ND parameters for all REEs simultaneously.

225 Unconstrained optimization of both $\log\tilde{K}$ and n for all REEs did not provide a good result (preliminary results not shown). Indeed, there was no expected trend in the $\log\tilde{K}_i$ values as observed in previous studies that showed at low REEs/HA ratios, when REEs bind to strong affinity sites, $\log K_i$ increases along the REE series from La to Lu (Marsac *et al.*, 2010; Yamamoto, Takahashi and Shimizu, 2010). Therefore, we followed the approach of Milne *et al.* (2003) to first
230 constrain the NICA non-ideality parameter n , using the LFER in which n for each metal is related to their first hydrolysis constant:

$$n_1 = 0.14 - 0.055 \log K_{OH} \quad (r^2 = 0.85) \quad (6)$$

$$n_2 = 0.76 n_1 \quad (7)$$

Using the latest REE hydrolysis constants $\log K_{OH}$ from Klungness & Byrne (2000), we applied
235 these equations to calculate n_i values for each of the REE and better constrain the fit. By this, we optimized only two parameters, the metal affinity constants $\log\tilde{K}_{i,1}$ and $\log\tilde{K}_{i,2}$.

Modelling the competition experiments

Competition of $\text{Al}^{3+}/\text{Fe}^{3+}/\text{Cu}^{2+}$ on REE-HA binding was modelled in ORCHESTRA (Meeussen, 2003), using default NICA-Donnan parameters (Milne *et al.*, 2003) and the Minteqv4
240 thermodynamic database (US-EPA, 1999). In the experimental set-up, precipitation of Al/Fe-hydroxides was expected at pH above 4.5 (Marsac *et al.*, 2012, 2013, 2021). This phenomenon was considered into the modelling by allowing precipitation of gibbsite ($\log K = -8.291$) and ferrihydrite ($\log K = -3.191$), respectively (Minteqv4 thermodynamic database).

Results and Discussion

245 **Determination of REE-specific affinity constants**

Obtained model parameters for the whole REEs series are given in **Table 2** and shown in black symbols in **Figure 1**. The $\log \tilde{K}_1$ pattern shows the expected downward concavity for the MREE (Marsac *et al.*, 2010; Yamamoto, Takahashi and Shimizu, 2010). The optimized parameters for Eu compare well with those derived by Milne *et al.* (2003) with $\log \tilde{K}_{i,1}$ being close to that derived by
250 Milne *et al.* (1.74 versus 1.92) but with somewhat higher $\log \tilde{K}_{i,2}$ than that obtained by Milne *et al.* (4.02 versus 3.43). These differences are possibly due to the use of partly other HAs in the study of Milne *et al.* compared to this study, together with the natural variation in binding constants amongst various humic substances (Groenenberg *et al.*, 2010). Differences for Dy are larger with $\log \tilde{K}_{i,1}$ of 1.4 and 0.8 and $\log \tilde{K}_{i,2}$ of 4.95 and 3.9 obtained in our study versus those of Milne *et al.*,
255 respectively. The parameters for Dy published by Milne *et al.* (2003) are, however, not very reliable as they are based on a very small data set for Dy binding to Aldrich HA with only six data points.

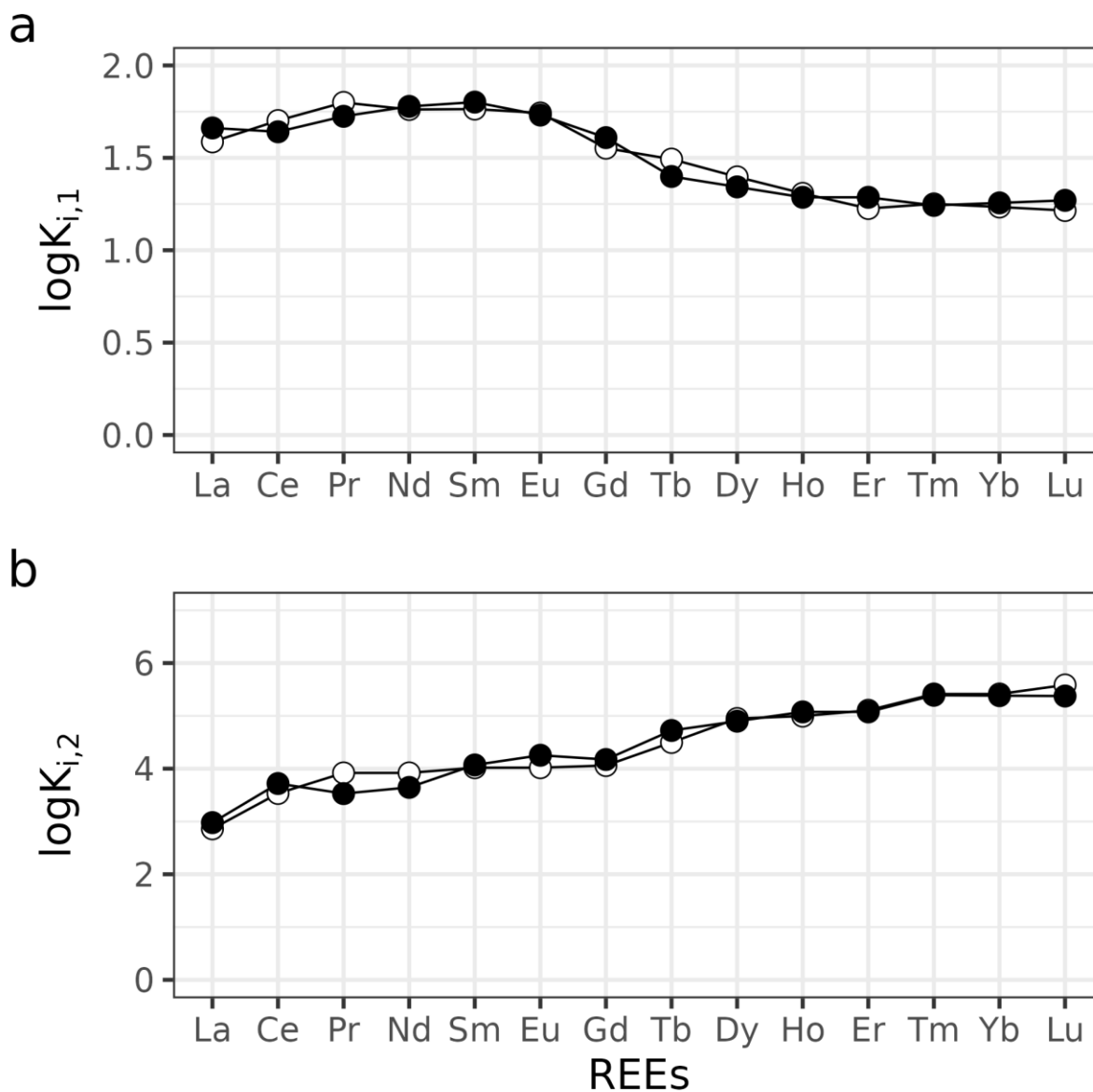


Figure 1. NICA-Donnan median affinity constants for each of the REE binding with the (a) type 1 (carboxylic) and (b) type 2 (phenolic) groups of HA. Black symbols were obtained by fitting the experimental datasets with PEST-ORCHESTRA; white symbols were obtained by calculating $\log \tilde{K}_i$ according to the Irving-Rossotti approach and optimized equation (8).

Table 2. Summary of REE-HA ND binding parameters, REE hydrolysis constants and the Irving-Rossotti coefficients for REE.

REE	$\log K_{OH}^a$	n_1^b	n_2^b	$\log \tilde{K}_{REE,1}^c$	$\log \tilde{K}_{REE,2}^c$	α_0^d	β_0^d
La	-8.81	0.62	0.47	1.59	2.86	0.30	1.02
Ce	-8.34	0.60	0.46	1.70	3.53	0.35	0.91
Pr	-8.32	0.60	0.45	1.80	3.92	0.34	0.99
Nd	-8.18	0.60	0.45	1.76	3.92	0.35	1.01
Sm	-7.84	0.57	0.43	1.76	4.02	0.38	0.97
Eu	-7.76	0.57	0.43	1.74	4.02	0.39	0.90
Gd	-7.83	0.57	0.43	1.55	4.06	0.38	0.83
Tb	-7.64	0.56	0.43	1.49	4.50	0.41	0.62
Dy	-7.59	0.56	0.42	1.40	4.95	0.42	0.56
Ho	-7.56	0.56	0.42	1.31	5.00	0.43	0.50
Er	-7.52	0.55	0.42	1.23	5.11	0.43	0.50
Tm	-7.39	0.55	0.42	1.25	5.41	0.45	0.43
Yb	-7.24	0.54	0.41	1.23	5.41	0.45	0.44
Lu	-7.27	0.54	0.41	1.21	5.58	0.45	0.45

265 ^a Klungness & Byrne (2000).

^b Calculated from equations (6) and (7), Milne *et al.* (2003)

^c Optimized using PEST-ORCHESTRA

^d Marsac *et al.* (2021)

Modelled REE-HA binding versus measurements for the four datasets used for the fitting are shown in **Figure 2**. Most data points fell into the 0.3 log unit envelope around the 1:1 line between measured and calculated REE-HA binding, which is comparable with results for other metals (Milne *et al.*, 2003) and indicative of a good fit. The relative importance of REE binding to type 1 carboxylic *versus* binding to type 2 phenolic sites decreases from the LREE to HREE (**Figure S1**). Electrostatic binding in the Donnan volume decreases with increasing pH and becomes insignificant above pH 5 (**Figure S1**).

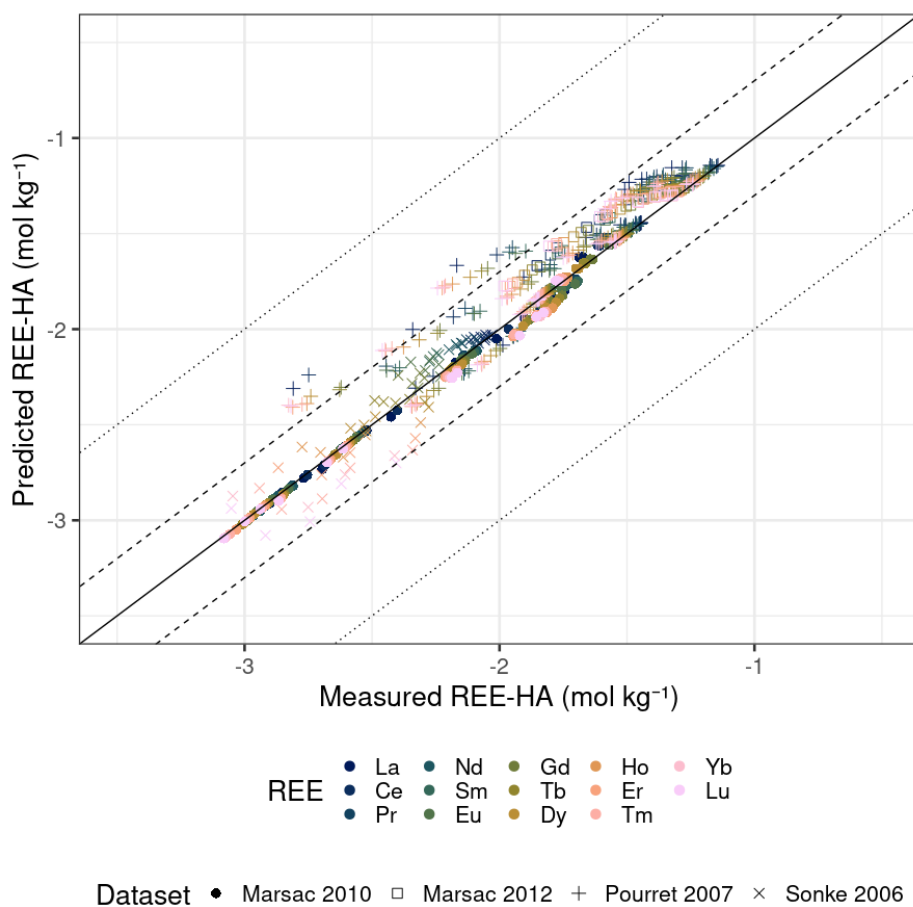


Figure 2. Comparison between predicted and measured HA-bound REEs for the four datasets. Dashed and dotted lines respectively represent the 0.3 and 1 log unit envelope around the 1:1 line.

Even though the four datasets, from which we derived the optimized model parameters, cover a wide pH range, we observe a trend of model residuals (i.e., the difference between model prediction and experimental measurement) with pH. The distribution of residuals shows the overprediction is largest at $\text{pH} \leq 3$ and decreases with increasing pH until pH 6, after which at higher pH the model increasingly underpredicts observations (**Figure S2**). This can also be seen in the results shown in **Figure 3**. With increasing pH, metal cations become increasingly hydrolysed. In addition to the binding of the free metal cations, hydrolysed cations possibly also bind specifically to the reactive sites of HA. Specific binding of hydrolysed species to HA is not taken into account in the ND model, this being different from Models VI and VII, for which specific adsorption of the first hydroxy species is included for all metal cations. In the NICA-Donnan model, hydrolysed species only interact with HA through electrostatic binding in the Donnan volume. Hydrolysis of REEs in the bulk solution starts to become important between about pH 7.3 for Lu, being the strongest hydrolysing lanthanide, and pH 8.8 for La (see $\log K_{\text{OH}}$ values in Table 2). Specific binding as modelled in the ND model is related to the local concentration of the metal cation in the Donnan volume, which is different from that in the bulk solution. According to equation (2), accumulation of the free trivalent species in the Donnan volume is stronger than that of the hydrolysed divalent and monovalent species. Speciation calculations for a fixed concentration of La and Lu in the bulk solution (**Figure S3**) show that the concentrations of hydrolysed species of Lu and La in the Donnan volume become important at higher pH values compared to that for the bulk solution, i.e., at pH values higher than 8.5 for Lu and even higher than 10 for La. In case specific binding of hydrolysed metal species is important for metal cation binding to HA, this is expected to be relevant only at pH values higher than 8.5 for the REE, especially the heavier REE (HREE). We indeed see relative large deviations between modelled

and measured binding for these HREE in the data from Sonke and Salters at pH 8.9 (Figure 3e).

300 However, similar deviations for these data were observed in the modelling with Model VII (Marsac et al., 2021), which in contrary with NICA includes specific binding of hydrolysed species.

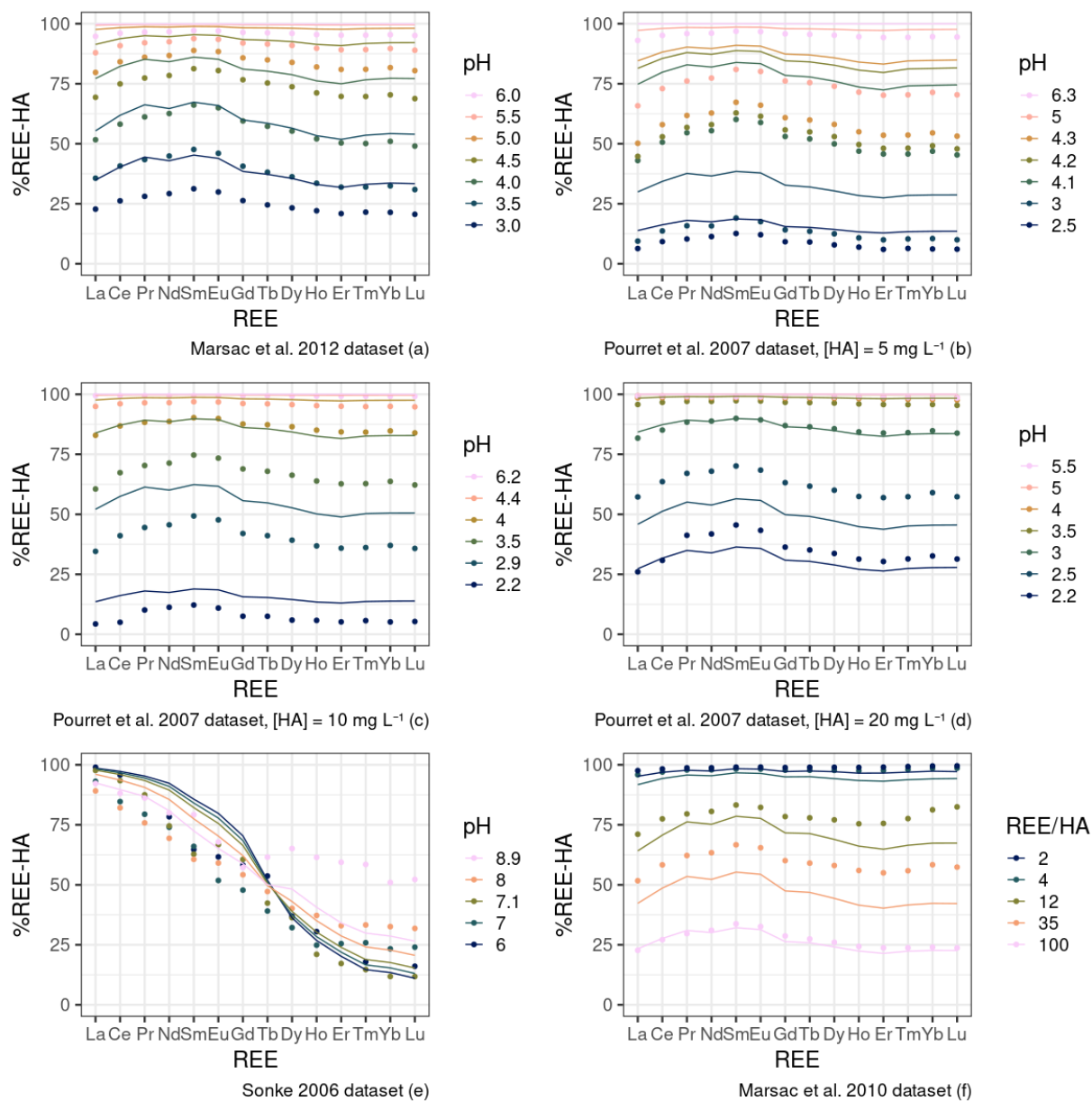


Figure 3. REE-HA patterns, shown as percentage of REE bound to HA of dataset from Marsac et al. (2012) (a), Pourret et al. (2007) (b-d), Sonke & Salters (2006) (e), Marsac et al. (2010) (f).

REE/HA values are given in mmol kg^{-1} , based on the La value for the whole series. Symbols are
305 experimental data and lines results of calculation.

Figure 3 shows the REE-HA pattern obtained for each of the parameterization datasets. The shape of this pattern is generally well described by the NICA-Donnan model. However, the effect of the REE/HA concentration ratio over the REE-HA binding prediction is not properly described by the
310 model for the data of Pourret *et al.* (2007), with REE-HA binding being overestimated at high REE/HA ratio (HA concentration = 5 mg L^{-1} , **Figure 3b**), and underestimated at the lowest REE/HA ratio (HA concentration = 20 mg L^{-1}) **Figure 3d**). Marsac *et al.* (2010) evidenced that at high metal loadings, REEs were bound through high-density low-affinity sites, whereas at low loadings strong affinity sites become more important. Our ND calculations indeed show a slight
315 increase in the REE binding with type 2 high affinity sites (phenolic type sites) with decreasing REE/HA ratio and *vice versa* an accompanying decrease in the binding to low affinity type 1 sites (carboxylic type sites) (**Figure S4**). This, however, did not lead to an accurate prediction of the REE/HA ratio dependent behaviour observed in the data from Pourret *et al.* (2007). Kouhail, Benedetti and Reiller (2016) evidenced that the fulvic acid (FA) concentration impacted Eu-FA
320 complexation using time-resolved luminescence spectroscopy. When increasing the FA concentration in solution, while keeping the concentration of Eu, pH and I at fixed levels, they observed the typical luminescence evolution of Eu complexed by humic substances in the low FA concentration range, but detected a second luminescence mode at higher FA concentrations. The first part - in the low FA concentration range - could be modelled adequately with the NICA-
325 Donnan model. The second part at higher FA concentrations is possibly related to interparticle binding, a process not included in present humic ion binding models such as Model VII, SHM or

NICA-Donnan. The FA concentration at which the luminescence pattern started to change decreased with increasing pH of the solution with the concentration of Suwannee River Fulvic Acid (C_{SRFA}) < 100 mg/L at pH 4, $C_{SRFA} < 40$ mg/L and $C_{SRFA} < 20$ mg/L at pH 7. This pH-
330 dependence may explain that REE binding to HA at different REE/HA ratios is well predicted by both ND (this study, **Figure 3f**) and Model VII (Marsac *et al.*, 2021) for the data of Marsac *et al.* (2010) that were measured at pH 3.

Model simulations by Marsac *et al.* (2021), who modelled the same data of Pourret *et al.* (2007)
335 using Model VII, show a similar trend as our ND simulations, with overestimation of REE-HA binding at low HA concentrations and underestimation of REE-HA binding at higher HA concentrations. The differences between their modelled concentrations at high and low HA concentrations are, however, less pronounced. An important difference in the experimental setup between Pourret *et al.* (2007) and Marsac *et al.* (2010) is I imposed by the concentration of the
340 background electrolyte NaNO_3 of 0.001 and 0.01 M respectively. The stronger deviations observed with the ND modelling compared to the simulations with Model VII at the low ionic strength for the Pourret *et al.* dataset may point into the direction of a discrepancy in the modelling of the electrostatic interactions, which would have a stronger effect with the lower I in the experiments of Pourret *et al.* compared to the experiments with the higher I of Marsac *et al.* (2010). According
345 to Koopal *et al.* (2022), and noted by Lenoir, Matynia and Manceau, (2010) and Janot *et al.* (2017), the use of equation (5) (Kinniburgh *et al.*, 1999), which relates the Donnan volume with the ionic strength, results in relatively strong electrostatic interactions. According to equation (2), a possible overestimation of the electrostatic potential will especially affect the electrostatic component in the binding of trivalent cations such as the REE, this because in the exponent of equation (2), the

350 valence of the ion z is multiplied with the electrostatic potential. At relatively high bulk concentrations as is the case with high REE/HA, this may lead to substantial overestimation of cation binding. It would be worthwhile to investigate the use of equation (4), which leads to more realistic potentials than the Kinniburgh-equation (5) (Janot *et al.*, 2017; Koopal *et al.*, 2022). . We, however, decided to stay with the one-parameter Kinniburgh equation (5) to have the newly
355 derived REE parameters compatible with the generic parameters of Milne *et al.* (2001, 2003), which are used as the default ND parameters in the chemical speciation software, ECOSAT, ORCHESTRA and Visual MINTEQ.

Comparison with Irving-Rossotti approach

Marsac *et al.* (2021) used another LFER than the one from Milne *et al.* (2003) to constrain their
360 REE-HA binding parameters. They followed the work of Irving and Rossotti (1956), who showed that the binding constant for monodentate binding of metals to oxygen ligands in organic acids (both carboxylic and phenolic) is related to the protonation constant of the ligand according to the linear correlation:

$$\log K_{ML} = \alpha_0 \log K_{HL} + \beta_0 \tag{8}$$

365 With $\log K_{HL}$ the equilibrium constant for proton-ligand formation, $\log K_{ML}$ the equilibrium constant for metal-ligand complexation, and α_0 and β_0 metal-specific parameters.

Applicability to the ND model

Carbonaro and DiToro (2007) showed that β_0 is close to zero for most elements and can be neglected. Together with Tipping *et al.* (2011), they used this LFER to regress the values of
370 $\log K_{MA}$, the mean equilibrium constant for metal binding to the stronger acid sites of NOM in the

WHAM humic ion binding models V, VI and VII. To investigate the possibility to apply this approach to the ND model, we regressed the ND median metal binding constants $\log\tilde{K}_1$ and $\log\tilde{K}_2$ for 11 metals that were obtained by Milne *et al.* (2003) without any constraints, against the Irving-Rossotti slope α_0 . Results are given in **Figure 4**, together with 9 other metals whose binding constants were also determined by Milne *et al.* (2003) by using constraints on the parameter optimisation. With the $\log\tilde{K}_1$ of Al clearly deviating from the linear relation, we excluded this metal from the regression, and obtained a good linear relationship, with R^2 of 0.89 and 0.90 for $\log\tilde{K}_1$ and $\log\tilde{K}_2$, respectively.

This observation allowed us to use the Irving-Rossotti approach to regularize ND parameters in a similar way as it was done for Model VII (Tipping, Lofts and Sonke, 2011; Marsac *et al.*, 2021).

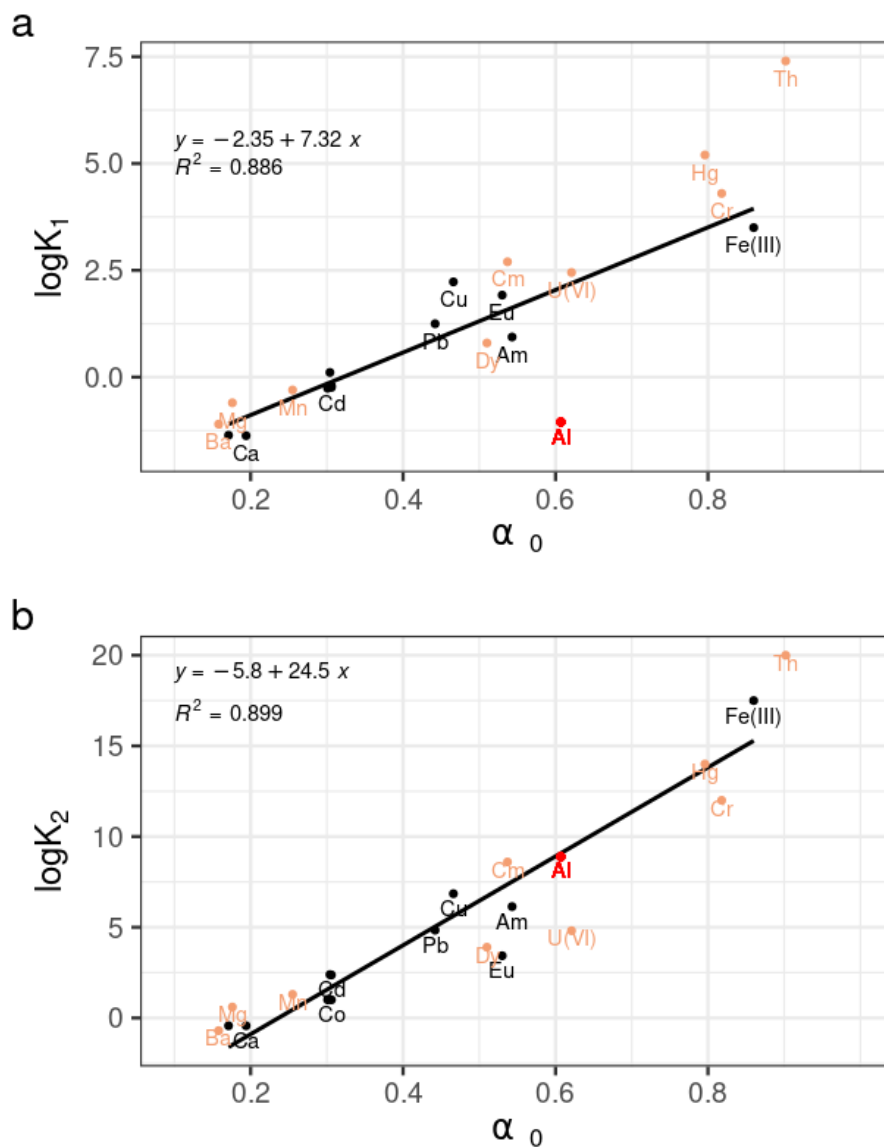


Figure 4 Generic NICA-Donnan parameters $\log \tilde{K}_1$ (a) and $\log \tilde{K}_2$ (b) against the corresponding Irving-Rossotti slope α_0 . Only the parameters determined by unconstrained optimization by Milne et al. (2003) are included in the linear regression ($n = 11$, black symbols). Note that Al is not included in the linear regression, due to large deviation of $\log \tilde{K}_{1,Al}$ from the other metal parameters (red symbols). Other metals for which data were available but for which generic $\log K_i$ were determined applying constrains on the fit are shown for comparison ($n = 9$, orange symbols).

385

Applicability to REEs

Carbonaro and DiToro (2007) found that β_0 significantly differed from 0 for several metal ions including Eu^{3+} . Later, Marsac *et al.* (2021) derived α_0 and β_0 values for the whole REEs series.

390 They found the following linear relation between LFER parameters (α_0 , β_0) and the binding constants $\log K_{MA}$ of REEs:

$$\log K_{M_i} = U_i \alpha_0 + V_i \beta_0 + W_i \quad (9),$$

where U_i , V_i and W_i are parameters that must be optimized for each type of binding sites.

Here, we fitted this LFER equation (9) to the above optimized $\log \tilde{K}_i$ values. For type 1 sites, we
395 obtained 2.71, 1.37 and -0.52 for U_1 , V_1 and W_1 , respectively. For type 2 sites, we obtained 13.20,
-0.74 and -0.24 for U_2 , V_2 and W_2 , respectively. As shown in **Figure 1** (grey symbols), the $\log \tilde{K}_i$
calculated using fitted equation (9) describe the patterns of the optimized $\log \tilde{K}_i$ rather well, which
gives confidence in the optimized ND parameters for REEs. These results also show the potential
to use the Irving-Rossotti approach to regularize existing NICA-Donnan parameters for other
400 metals.

Prediction of cation-competition effect on REE-HA binding

Modelling the effect of competitive cation binding (Fe^{3+} , Al^{3+} , Cu^{2+}) on REE binding to HA was performed using experimental datasets previously published (Marsac *et al.*, 2012, 2013, 2021).

Metal-binding parameters used were the generic ND parameters (Milne *et al.*, 2003), reminded in

405 **Table S1.**

The modelled and measured pH-edge impact of parameterization on REE binding to HA is displayed in **Figure 5** for Eu. Results show that, using generic parameters, binding of Eu to HA is over-predicted at all pH in the absence and in presence for all competitors. Experimental results

show no effect of Cu^{2+} on REE-HA binding, contrary to the trivalent Al^{3+} and Fe^{3+} which, when
 410 present in the system, lead to a significant decrease in REE-HA binding.

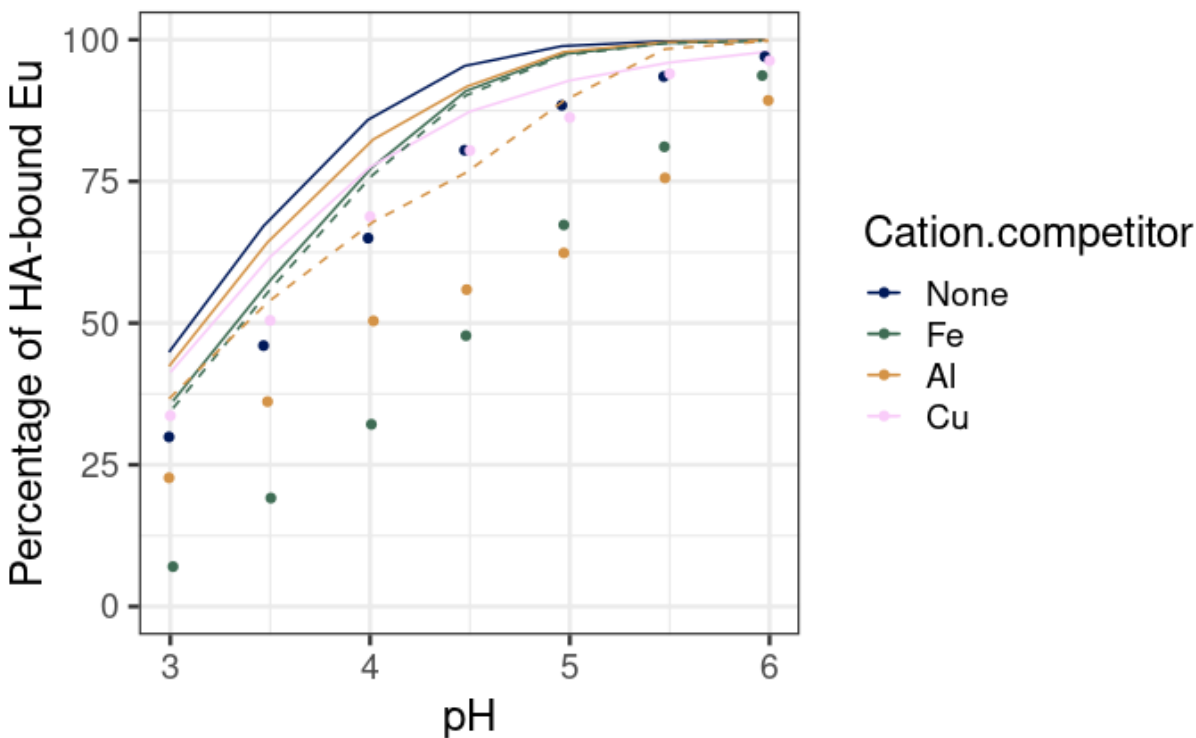


Figure 5. pH-edge of Eu binding to HA, depending on the competitor present (Fe^{3+} , Al^{3+} , Cu^{2+} or none). Points are experimental results (Marsac et al. 2021) and lines are model predictions: solid lines with generic parameters and dashed lines with updated parameters according to the IR approach and regression given in Figure 4.

415

The use of the generic NICA-Donnan model parameters from Milne *et al.* (2003) to describe this competition effect seems to have quite strong limitations, since the addition of the three cations in the modelling only leads to a slight decrease in the calculated amount of Eu-HA binding. We thus used the LFER determined above (**Figure 4**) to update the Fe and Al NICA-Donnan parameters
 420 proposed by Milne *et al.* (2003): $\log\tilde{K}_{1,\text{Fe}}$ was shifted from 3.5 to 3.95, $\log\tilde{K}_{1,\text{Al}}$ from -1.05 to 2.09 and $\log\tilde{K}_{2,\text{Al}}$ from 8.89 to 9.07. Results on the binding of Eu to HA are shown in **Figure 5**. The slight increase of $\log\tilde{K}_{1,\text{Fe}}$ has no impact on Eu nor on Fe binding (**Figure S5**). However, the

substantial increase of $\log\tilde{K}_{1,Al}$ has a significant impact on Al complexation to HA (**Figure S5**), and thus on REEs binding, as shown in **Figure 5** for Eu, although Eu complexation is still over-
425 estimated for the whole pH range studied.

This over-estimation of REE binding to HA by the ND model across a large range of pH values, even in the presence of competitors, could be possibly due to the generic site densities Q_i of Milne *et al.* (2003) being too high for the specific HA (PAHA) used in this study. Adapting of proton-binding parameters to the specific HA used in these experiments could be a way to increase the
430 accuracy of the results. However, it has not been tested since this was out of scope of this study. Indeed, the goal of this work was to determine generic REE-HA binding parameters compatible with the generic parameters of Milne *et al.* (2003) that can be applied in a wide range of environmental conditions (type of HA as well as pH, ionic strength or REE/HA concentrations), to be able to predict REE behaviour in such environments. We consistently capture the shapes of
435 REEs patterns and the impact of various environmental parameters, which can give us confidence in the derived parameters.

Another explanation of the discrepancies between experimental and modelling results of the competition experiments could be due to the fact that the specific binding of the Al- and Fe hydroxyl species ($AlOH^{2+}$, $FeOH^{2+}$) to HA is not taken into account in the ND model. In the
440 present ND model, these hydrolysed species only interact with HA through electrostatic binding in the Donnan volume. Including the specific binding of hydroxy species in ND as within Model VII, is worthwhile to consider as the modelling of strong hydrolysing trivalent species (e.g., Al, Fe) with NICA-Donnan is known to be inferior compared to the modelling of the less strongly hydrolysing divalent species (Milne *et al.*, 2003).

445 **Conclusions**

Recently, several datasets from literature were collected to calibrate the advanced humic-ion binding model for the prediction of REE binding to HA Model VII (Marsac *et al.*, 2021). This work provides parameters to model REE binding to HA in various physico-chemical conditions of pH, concentrations and ionic strengths, in the framework of another advanced humic-ion binding
450 model, the NICA-Donnan model. At the moment, such advanced models are the best option to predict metal ion binding to HS (Koopal, Tan and Avena, 2020). This work will thus make it possible to calculate REE speciation in various environments with ND using chemical speciation software (ECOSAT, ORCHESTRA, and Visual MINTEQ).

This work also evidenced the potential of the Irving-Rossotti approach to estimate and constrain
455 metal-binding parameters for the NICA-Donnan model. Here we showed that it can also be applied for ND parameter estimation of REEs when using the extended Irving Rosotti approach (Marsac *et al.*, 2021).

Acknowledgments

This work was supported by the French National Research Agency through the national program
460 ‘Investissements d’avenir’, reference ANR-10LABX-21–01/LABEX RESSOURCES 21). This manuscript benefited from the constructive comments of two anonymous reviewers.

Conflicts of Interest

The authors declare no conflicts of interest.

Data availability

465 This paper contained no new or unpublished data.

CRedit author statement

A. Otero-Fariña: Conceptualization, Investigation, Formal analysis, Writing - Original Draft;

N. Janot: Conceptualization, Investigation, Visualization, Writing – Original Draft; Writing - Review & Editing;

470 **R. Marsac:** Resources, Writing - Review & Editing;

C. Catrouillet: Writing - Review & Editing;

J.E. Groenberg: Conceptualization, Methodology, Investigation, Resources, Writing - Review & Editing, Supervision

References

- Batley, G.E. *et al.* (2022) 'Metal contaminants of emerging concern in aquatic systems', *Environmental Chemistry*, 19(1), pp. 23–40. Available at: <https://doi.org/10.1071/EN22030>.
- Benedetti, M.F., Van Riemsdijk, W.H. and Koopal, L.K. (1996) 'Humic Substances Considered as a Heterogeneous Donnan Gel Phase', *Environmental Science & Technology*, 30(6), pp. 1805–1813. Available at: <https://doi.org/10.1021/es950012y>.
- Borgmann, U. *et al.* (2005) 'Toxicity of sixty-three metals and metalloids to *Hyalella azteca* at two levels of water hardness', *Environmental Toxicology and Chemistry*, 24(3), pp. 641–652. Available at: <https://doi.org/10.1897/04-177R.1>.
- Carbonaro, R.F. and Di Toro, D.M. (2007) 'Linear free energy relationships for metal–ligand complexation: Monodentate binding to negatively-charged oxygen donor atoms', *Geochimica et Cosmochimica Acta*, 71(16), pp. 3958–3968. Available at: <https://doi.org/10.1016/j.gca.2007.06.005>.
- Catrouillet, C. *et al.* (2019) 'Rare earth elements as tracers of active colloidal organic matter composition', *Environmental Chemistry*, 17(2), pp. 133–139. Available at: <https://doi.org/10.1071/EN19159>.
- Di Bonito, M., Lofts, S. and Groenenberg, J.E. (2018) 'Models of Geochemical Speciation: Structure and Applications', in *Environmental Geochemistry: Site Characterization, Data Analysis and Case Histories*. Elsevier, pp. 237–305. Available at: <https://doi.org/10.1016/B978-0-444-63763-5.00012-4>.
- Gangloff, S. *et al.* (2014) 'Characterization and evolution of dissolved organic matter in acidic forest soil and its impact on the mobility of major and trace elements (case of the Strengbach watershed)', *Geochimica et Cosmochimica Acta*, 130, pp. 21–41. Available at: <https://doi.org/10.1016/j.gca.2013.12.033>.
- Gonzalez, V. *et al.* (2014) 'Environmental fate and ecotoxicity of lanthanides: Are they a uniform group beyond chemistry?', *Environment international*, 71, pp. 148–57. Available at: <https://doi.org/10.1016/j.envint.2014.06.019>.
- González, V. *et al.* (2015) 'Lanthanide ecotoxicity: First attempt to measure environmental risk for aquatic organisms', *Environmental Pollution*, 199, pp. 139–147. Available at: <https://doi.org/10.1016/j.envpol.2015.01.020>.

- 475 Groenenberg, J.E., Koopmans, G., Comans, R.N.J. (2010) ‘Uncertainty Analysis of the Nonideal Competitive Adsorption–Donnan Model: Effects of Dissolved Organic Matter Variability on Predicted Metal Speciation in Soil Solution’, *Environmental Science and Technology*, 44(4), pp.1340–1346. Available at: <https://doi.org/10.1021/es902615w>
- Groenenberg, J.E. and Lofts, S. (2014) ‘The use of assemblage models to describe trace element partitioning, speciation, and fate: A review’, *Environmental Toxicology and Chemistry*, 33(10), pp. 2181–2196. Available at: <https://doi.org/10.1002/etc.2642>.
- Gustafsson, J.P. (2001) ‘Modeling the Acid–Base Properties and Metal Complexation of Humic Substances with the Stockholm Humic Model’, *Journal of Colloid and Interface Science*, 244(1), pp. 102–112. Available at: <https://doi.org/10.1006/jcis.2001.7871>.
- Gwenzi, W. *et al.* (2018) ‘Sources, behaviour, and environmental and human health risks of high-technology rare earth elements as emerging contaminants’, *Science of The Total Environment*, 636, pp. 299–313. Available at: <https://doi.org/10.1016/j.scitotenv.2018.04.235>.
- Irving, H. *et al.* (1956) ‘Some Relationships Among the Stabilities of Metal Complexes.’, *Acta Chemica Scandinavica*, 10, pp. 72–93. Available at: <https://doi.org/10.3891/acta.chem.scand.10-0072>.
- Janot, N. *et al.* (2017) ‘PEST-ORCHESTRA, a tool for optimising advanced ion-binding model parameters: derivation of NICA-Donnan model parameters for humic substances reactivity’, *Environmental Chemistry*, 14(1), p. 31. Available at: <https://doi.org/10.1071/EN16039>.
- Johannesson, K.H. *et al.* (2004) ‘Rare earth element concentrations and speciation in organic-rich blackwaters of the Great Dismal Swamp, Virginia, USA’, *Chemical Geology*, 209(3–4), pp. 271–294. Available at: <https://doi.org/10.1016/j.chemgeo.2004.06.012>.
- Khan, A.M. *et al.* (2016) ‘Assessing anthropogenic levels, speciation, and potential mobility of rare earth elements (REEs) in ex-tin mining area’, *Environmental Science and Pollution Research*, 23(24), pp. 25039–25055. Available at: <https://doi.org/10.1007/s11356-016-7641-x>.
- Kinniburgh, D.G. *et al.* (1999) ‘Ion binding to natural organic matter: competition, heterogeneity, stoichiometry and thermodynamic consistency’, *Colloids and Surfaces A: Physicochemical and Engineering Aspects*, 151(1–2), pp. 147–166. Available at: [https://doi.org/10.1016/S0927-7757\(98\)00637-2](https://doi.org/10.1016/S0927-7757(98)00637-2).
- Klungness, G.D. and Byrne, R.H. (2000) ‘Comparative hydrolysis behavior of the rare earths and yttrium: the influence of temperature and ionic strength’, *Polyhedron*, 19(1), pp. 99–107. Available at: [https://doi.org/10.1016/S0277-5387\(99\)00332-0](https://doi.org/10.1016/S0277-5387(99)00332-0).
- Koopal, L. *et al.* (2022) ‘Proton binding to humic nano particles: electrostatic interaction and the condensation approximation’, *Physical Chemistry Chemical Physics*, 24(2), pp. 704–714. Available at: <https://doi.org/10.1039/D1CP04470B>.

Koopal, L., Tan, W. and Avena, M. (2020) 'Equilibrium mono- and multicomponent adsorption models: From homogeneous ideal to heterogeneous non-ideal binding', *Advances in Colloid and Interface Science*, 280, p. 102138. Available at: <https://doi.org/10.1016/j.cis.2020.102138>.

Koopal, L.K. *et al.* (2005) 'Ion binding to natural organic matter: General considerations and the NICA–Donnan model', *Colloids and Surfaces A: Physicochemical and Engineering Aspects*, 265(1–3), pp. 40–54. Available at: <https://doi.org/10.1016/j.colsurfa.2004.11.050>.

Kouhail, Y., Dror, I. and Berkowitz, B. (2019) 'Current knowledge on transport and reactivity of technology-critical elements (TCEs) in soil and aquifer environments', *Environmental Chemistry* [Preprint]. Available at: <https://doi.org/10.1071/EN19102>.

Kouhail, Y. Benedetti, M.F. and Reiller, P.E. (2016) 'Eu(III)–Fulvic Acid Complexation: Evidence of Fulvic Acid Concentration Dependent Interactions by Time-Resolved Luminescence Spectroscopy' *Environmental Science & Technology*, 50 (7), pp. 3706–3713. Available at <https://doi.org/10.1021/acs.est.5b05456>

Lachaux, N. *et al.* (2022) 'Implications of speciation on rare earth element toxicity: A focus on organic matter influence in *Daphnia magna* standard test', *Environmental Pollution*, 307, p. 119554. Available at: <https://doi.org/10.1016/j.envpol.2022.119554>.

Lenoir, T., Matynia, A. and Manceau, A. (2010) 'Convergence-optimized procedure for applying the NICA–Donnan model to potentiometric titrations of humic substances', *Environmental Science and Technology*, 44(16), pp. 6221–6227. Available at: <https://doi.org/10.1021/es1015313>.

Leybourne, M.I. and Johannesson, K.H. (2008) 'Rare earth elements (REE) and yttrium in stream waters, stream sediments, and Fe–Mn oxyhydroxides: Fractionation, speciation, and controls over REE+Y patterns in the surface environment', *Geochimica et Cosmochimica Acta*, 72(24), pp. 5962–5983. Available at: <https://doi.org/10.1016/j.gca.2008.09.022>.

Liu, H. *et al.* (2017) 'Rare earth elements sorption to iron oxyhydroxide: Model development and application to groundwater', *Applied Geochemistry*, 87, pp. 158–166. Available at: <https://doi.org/10.1016/j.apgeochem.2017.10.020>.

Lofts, S. and Tipping, E. (2011) 'Assessing WHAM/Model VII against field measurements of free metal ion concentrations: Model performance and the role of uncertainty in parameters and inputs', *Environmental Chemistry*, 8(5), pp. 501–516. Available at: <https://doi.org/10.1071/EN11049>.

Malhotra, N. *et al.* (2020) 'An Updated Review of Toxicity Effect of the Rare Earth Elements (REEs) on Aquatic Organisms', *Animals*, 10(9), p. 1663. Available at: <https://doi.org/10.3390/ani10091663>.

Marsac, R. *et al.* (2010) 'Metal loading effect on rare earth element binding to humic acid: Experimental and modelling evidence', *Geochimica et Cosmochimica Acta*, 74(6), pp. 1749–1761. Available at: <https://doi.org/10.1016/j.gca.2009.12.006>.

Marsac, R. *et al.* (2011) ‘An improved description of the interactions between rare earth elements and humic acids by modeling: PHREEQC-Model VI coupling’, *Geochimica et Cosmochimica Acta*, 75(19), pp. 5625–5637. Available at: <https://doi.org/10.1016/j.gca.2011.07.009>.

Marsac, R. *et al.* (2012) ‘Aluminium competitive effect on rare earth elements binding to humic acid’, *Geochimica et Cosmochimica Acta*, 89, pp. 1–9. Available at: <https://doi.org/10.1016/j.gca.2012.04.028>.

Marsac, R. *et al.* (2013) ‘Effects of Fe competition on REE binding to humic acid: Origin of REE pattern variability in organic waters’, *Chemical Geology*, 342, pp. 119–127. Available at: <https://doi.org/10.1016/j.chemgeo.2013.01.020>.

Marsac, R. *et al.* (2021) ‘Modeling rare earth elements binding to humic acids with model VII’, *Chemical Geology*, 567, p. 120099. Available at: <https://doi.org/10.1016/j.chemgeo.2021.120099>.

Meeussen, J.C.L. (2003) ‘ORCHESTRA: An Object-Oriented Framework for Implementing Chemical Equilibrium Models’, *Environmental Science & Technology*, 37(6), pp. 1175–1182. Available at: <https://doi.org/10.1021/es025597s>.

Migaszewski, Z.M. and Galuszka, A. (2015) ‘The Characteristics, Occurrence, and Geochemical Behavior of Rare Earth Elements in the Environment: A Review’, *Critical Reviews in Environmental Science and Technology*, 45(5), pp. 429–471. Available at: <https://doi.org/10.1080/10643389.2013.866622>.

Milne, C.J. *et al.* (2003) ‘Generic NICA–Donnan Model Parameters for Metal-Ion Binding by Humic Substances’, *Environmental Science & Technology*, 37(5), pp. 958–971. Available at: <https://doi.org/10.1021/es0258879>.

Milne, C.J., Kinniburgh, D.G. and Tipping, E. (2001) ‘Generic NICA-Donnan Model Parameters for Proton Binding by Humic Substances’, *Environmental Science & Technology*, 35(10), pp. 2049–2059. Available at: <https://doi.org/10.1021/es000123j>.

Oral, R. *et al.* (2017) ‘Heavy rare earth elements affect early life stages in *Paracentrotus lividus* and *Arbacia lixula* sea urchins’, *Environmental Research*, 154, pp. 240–246. Available at: <https://doi.org/10.1016/j.envres.2017.01.011>.

Pagano, G. *et al.* (2019) ‘Human exposures to rare earth elements: Present knowledge and research prospects’, *Environmental Research*, 171, pp. 493–500. Available at: <https://doi.org/10.1016/j.envres.2019.02.004>.

Pourret, O. *et al.* (2007) ‘Rare earth elements complexation with humic acid’, *Chemical Geology*, 243(1–2), pp. 128–141. Available at: <https://doi.org/10.1016/j.chemgeo.2007.05.018>.

Pourret, O. *et al.* (2010) ‘Colloidal Control on the Distribution of Rare Earth Elements in Shallow Groundwaters’, *Aquatic Geochemistry*, 16(1), pp. 31–59. Available at: <https://doi.org/10.1007/s10498-009-9069-0>.

US-EPA, MINTEQA2/PRODEFA2, A Geochemical assessment model for environmental

480 *systems: user manual supplement for version 4.0; US-EPA, National Exposure Research Laboratory, Ecosystems Research Division: Athens, GA, 1999.*

van Riemsdijk, W.H. *et al.* (2006) ‘Modeling the Interactions between Humics, Ions, and Mineral Surfaces †’, *Environmental Science & Technology*, 40(24), pp. 7473–7480. Available at: <https://doi.org/10.1021/es0607786>.

Romero-Freire, A. *et al.* (2018) ‘Assessment of baseline ecotoxicity of sediments from a prospective mining area enriched in light rare earth elements’, *Science of The Total Environment*, 612, pp. 831–839. Available at: <https://doi.org/10.1016/j.scitotenv.2017.08.128>.

Romero-Freire, A. *et al.* (2019) ‘Assessment of the toxic effects of mixtures of three lanthanides (Ce, Gd, Lu) to aquatic biota’, *Science of The Total Environment*, 661, pp. 276–284. Available at: <https://doi.org/10.1016/j.scitotenv.2019.01.155>.

Romero-Freire, A. *et al.* (2021) ‘Cytotoxicity and genotoxicity of lanthanides for *Vicia faba* L. are mediated by their chemical speciation in different exposure media’, *Science of The Total Environment*, 790, p. 148223. Available at: <https://doi.org/10.1016/j.scitotenv.2021.148223>.

Singhal, R.K. *et al.* (2006) ‘The use of ultra filtration in trace metal speciation studies in sea water’, *Environment International*, 32(2), pp. 224–228. Available at: <https://doi.org/10.1016/j.envint.2005.08.015>.

Sonke, J.E. and Salters, V.J.M. (2006) ‘Lanthanide–humic substances complexation. I. Experimental evidence for a lanthanide contraction effect’, *Geochimica et Cosmochimica Acta*, 70(6), pp. 1495–1506. Available at: <https://doi.org/10.1016/j.gca.2005.11.017>.

Tipping, E. (1998) ‘Humic Ion-Binding Model VI: An Improved Description of the Interactions of Protons and Metal Ions with Humic Substances’, *Aquatic Geochemistry*, 4, pp. 3–48.

Tipping, E. (2002) *Cation Binding by Humic Substances*. Cambridge: Cambridge University Press (Cambridge Environmental Chemistry Series). Available at: <https://doi.org/10.1017/CBO9780511535598>.

Tipping, E., Lofts, S. and Sonke, J.E. (2011) ‘Humic Ion-Binding Model VII: a revised parameterisation of cation-binding by humic substances’, *Environmental Chemistry*, 8(3), p. 225. Available at: <https://doi.org/10.1071/EN11016>.

Vermeer, A.W.P., van Riemsdijk, W.H. and Koopal, L.K. (1998) ‘Adsorption of Humic Acid to Mineral Particles. 1. Specific and Electrostatic Interactions’, *Langmuir*, 14(10), pp. 2810–2819. Available at: <https://doi.org/10.1021/la970624r>.

Vukov, O., Smith, D.S. and McGeer, J.C. (2016) ‘Acute dysprosium toxicity to *Daphnia pulex* and *Hyalella azteca* and development of the biotic ligand approach’, *Aquatic Toxicology*, 170, pp. 142–151. Available at: <https://doi.org/10.1016/j.aquatox.2015.10.016>.

Yamamoto, Y., Takahashi, Y. and Shimizu, H. (2010) 'Systematic change in relative stabilities of REE-humic complexes at various metal loading levels', *Geochemical Journal*, 44(1), pp. 39–63. Available at: <https://doi.org/10.2343/geochemj.1.0041>.

SUPPLEMENTARY INFORMATION

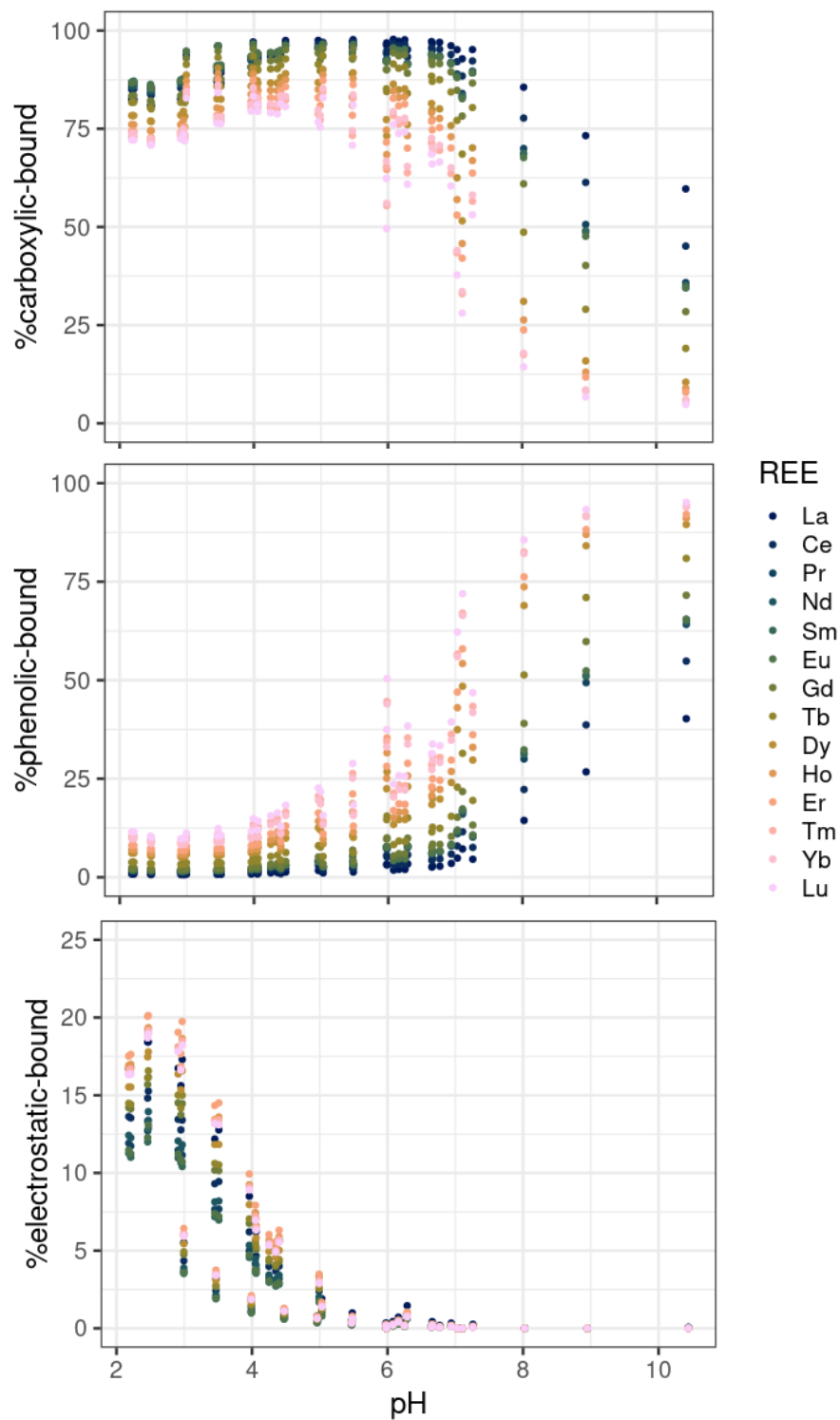
485 Rare Earth Elements complexation to humic
acids: NICA-Donnan model
parameterization

490

Alba Otero-Fariña^{1,a}, Noémie Janot^{1,2,3}, Rémi Marsac⁴, Charlotte
Catrouillet⁵, Jan E. Groenenberg^{1,6}

Table S1. NICA-Donnan binding parameters obtained in the literature modelled for generic HA, for proton and competitor metals.

Ion	H ⁺		Fe ³⁺		Al ³⁺		Cu ²⁺
	Generic (<i>Milne et al., 2003</i>)	Generic (<i>Milne et al., 2003</i>)	Adapted from LFER (this study)	Generic (<i>Milne et al., 2003</i>)	Adapted from LFER (this study)	Generic (<i>Milne et al., 2003</i>)	
b	0.49						
Q _{max,1} (eq/kg)	3.15						
Q _{max,2} (eq/kg)	2.55						
p ₁	0.62						
p ₂	0.41						
log $\tilde{K}_{i,1}$	2.93	3.5	3.95	-1.05	2.09		2.23
log $\tilde{K}_{i,2}$	8.00	17.5		8.89	9.07		6.85
n _{i,1}	0.81	0.30		0.40			0.56
n _{i,2}	0.63	0.25		0.30			0.34



500

Figure S1. Predicted speciation of REEs bound to HA as a function of pH. Marsac 2010 dataset was excluded from the plot for the sake of clarity, due to the limited pH range of these experiments, performed in different conditions.

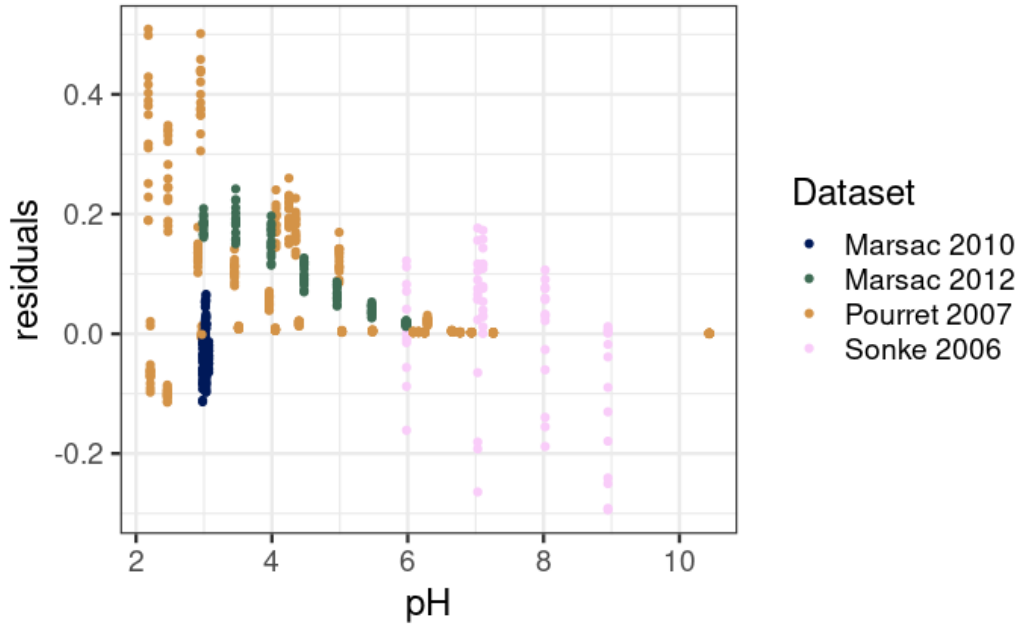
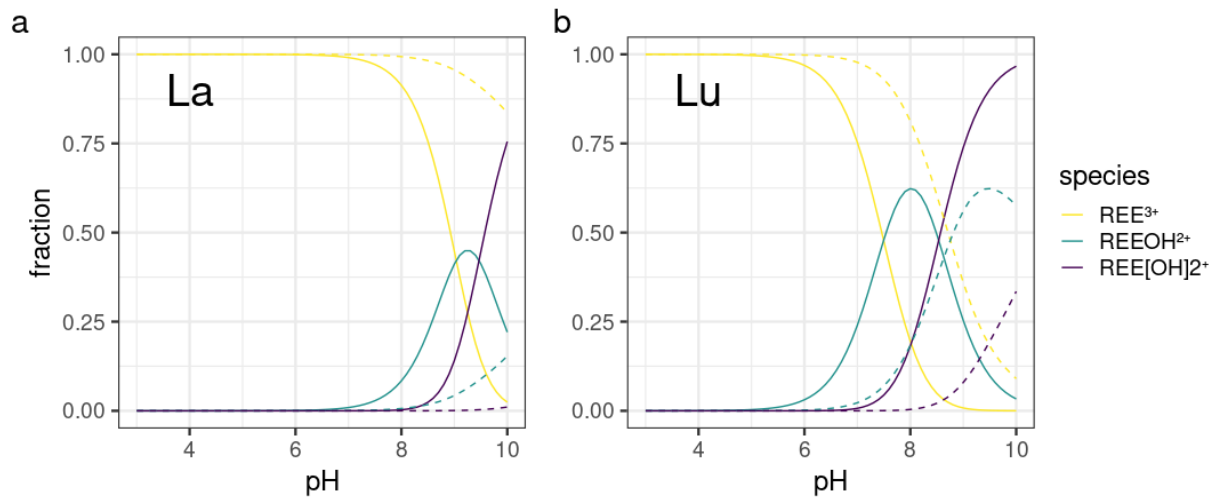


Figure S2. Residuals distribution of parameterization dataset as a function of solution pH and original dataset.



510 Figure S3. Calculated speciation of La (left) and Lu (right) in bulk solution (solid lines) and in the Donnan volume (dashed lines) using generic HA binding parameters.

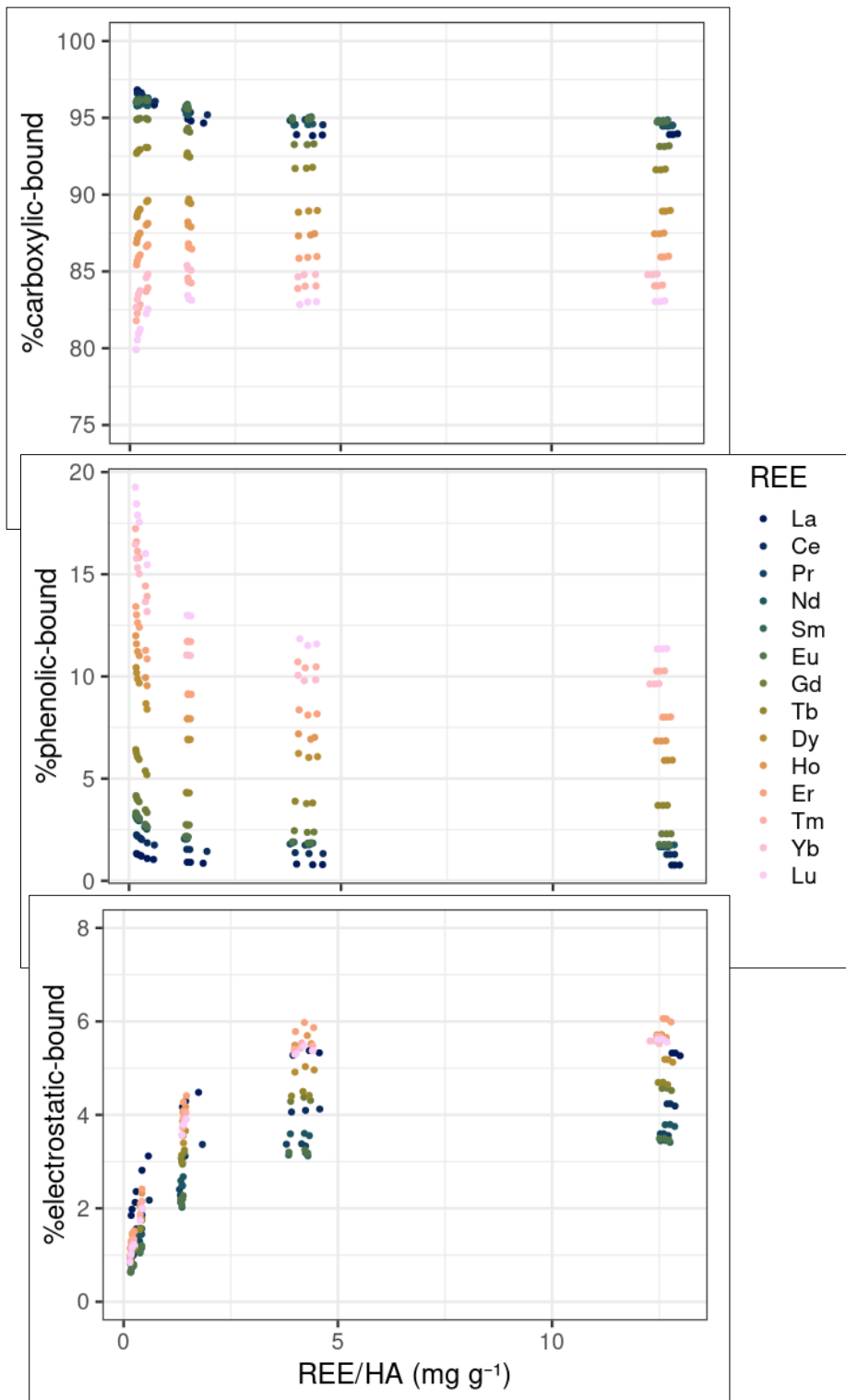


Figure S4. Predicted speciation of REEs bound to HA as a function of REE/HA ratio for the Marsac et al. 2010 dataset.

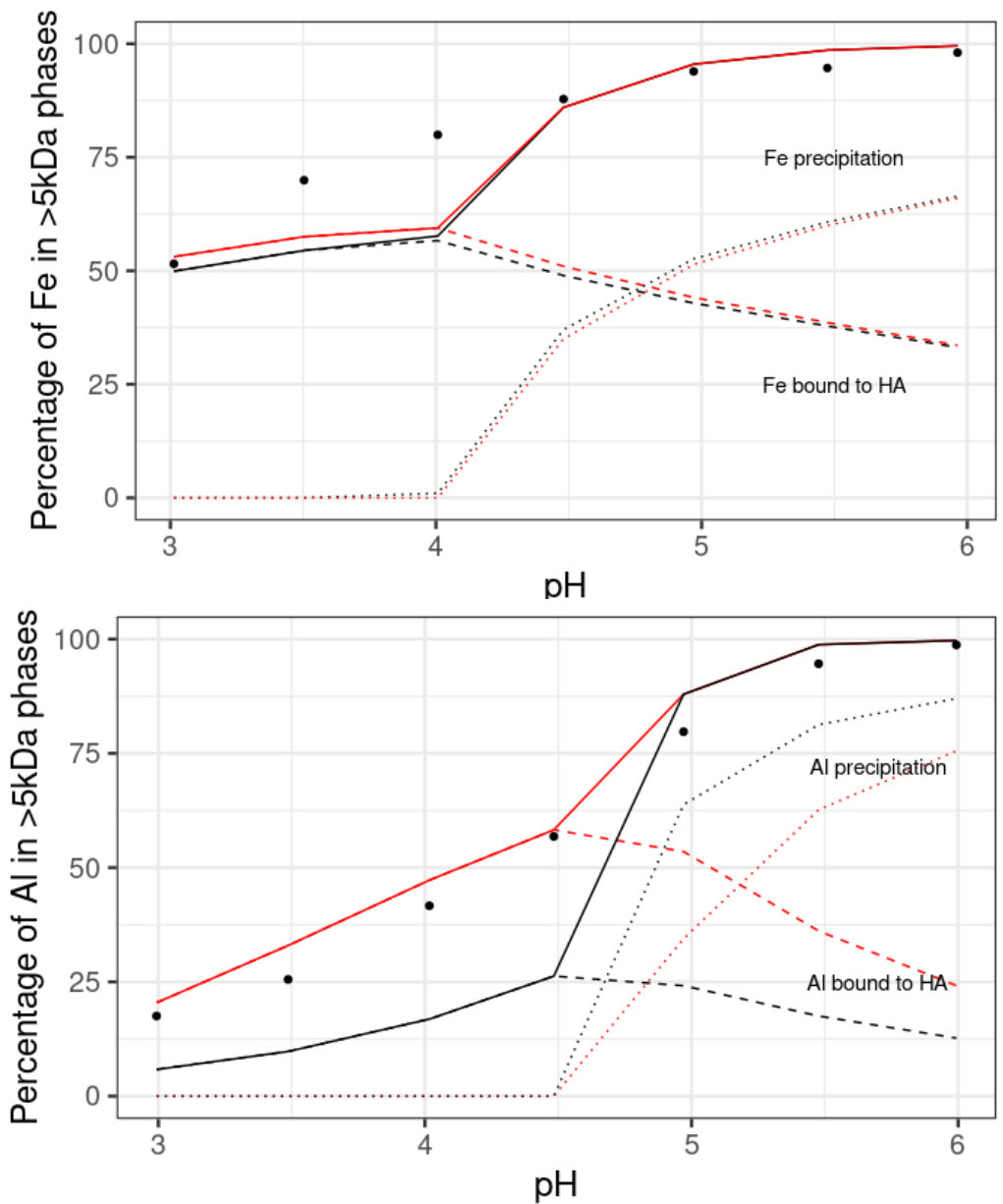


Figure S5. Percentage of Fe(III) (top) or Al(III) (bottom) retained by a 5 kDa filter versus pH in presence of REE, as experimentally determined (symbols) or calculated (lines) for $[HA] = 12 \text{ mg L}^{-1}$, $\sum[REE] = [Al/Fe] = 10 \mu\text{M}$ in 0.01 M NaCl . Black lines correspond to default generic parameters, red lines to Fe/Al parameters adapted according to the LFER given in Figure 4.